Chemistry and Physics of Lipids, 54 (1990) 193—203
Elsevier Scientific Publishers Ireland Ltd.

Polymorphic phase behavior of alpha-tocopherol hemisuccinate

Lawrence T. Boni[a], Walter R. Perkins[a], Sharma R. Minchey[a], Lois E. Bolcsak[a], Sol M. Gruner[b], Pieter R. Cullis[c,d], Michael J. Hope[c] and Andrew S. Janoff[a]

[a]The Liposome Company, Inc., 1 Research Way, Princeton, NJ 08540 (U.S.A.), [b]Princeton University, Department of Physics, John Henry Laboratories, P.O. Box 708, Princeton, NJ 08544 (U.S.A.), [c]The Canadian Liposome Company, Ltd., Suite 308, 267 West Esplanade, North Vancouver, British Columbia V7M 1A5 (Canada) and [d]The University of British Columbia, 2146 Health Sciences Mall, Vancouver, British Columbia V6T 1W5 (Canada)

(Received October 26th, 1989; revision received and accepted January 2nd, 1990)

From freeze-fracture electron microscopy and x-ray diffraction we show that α-tocopherol hemisuccinate (α -THS) is capable of polymorphic phase behavior, including the formation of the hexagonal II phase. The transition from bilayer to hexagonal phase was induced by changes in pH, the addition of Ca^{2+}, or the inclusion of tocopherol. Non-bilayer phases were found to begin below pH 7.5 with hexagonal phase predominating at pH 6.0 and below. The presence of tocopherol at 30 mol% at pH values otherwise favoring the bilayer phase was marked by the appearance of lipidic particles which gave way to purely hexagonal phase at 50 mol%. Ca^{2+} added at pH 7.5 induced a complex mixture of dehydrated lamellar and hexagonal II phases. The kinetics of the pH induced transition, as determined by NBD-PE fluorescence and freeze-fracture electron microscopy, were rapid and increased with increasing temperature and decreasing vesicle size.

Keywords: liposomes; non-bilayer phases; hexagonal phases; X-ray diffraction; freeze-fracture electron microscopy.

Introduction

Alpha-tocopherol hemisuccinate (α-THS), when dispersed in buffer at neutral pH, forms liposomes of multilamellar character [1—3]. These vesicles arise spontaneously, yield high trapping efficiencies and produce broad, ill defined low angle X-ray diffraction patterns consistent with systems possessing weak interlamellar forces [1]. Although most freeze-fracture replicas of these vesicles reveal smooth fracture faces, we have occasionally encountered systems with local disturbances in the bilayer organization reminiscent of lipidic particles. The existence of such structures has been associated with lipids having the capacity to form extended non-bilayer arrays. Particularly in systems with a net negative charge (such as α-THS), this capacity has been favored under conditions leading to charge neutralization [4]. Accordingly, we investigated the effect of pH and the presence of cations on the polymorphic phase behavior of α-THS. We report here that at pH values below 7.5 α-THS in pure form can, in fact, adopt non-bilayer structures. The kinetics of the pH transition were rapid and increased as temperature was increased or as vesicle size decreased. The addition of Ca^{2+} at neutral and basic pH values resulted in non-bilayer structures that were different from those induced by low pH. Further, the addition of tocopherol at greater than 30 mole percent at pH values otherwise favoring

Correspondence to: Andrew Janoff.

Abbreviations: DOPC, dioleoylphosphatidylcholine; DOPE, dioleoylphosphatidylethanolamine; 7-DS, 7-doxyl stearate; EPR, electron paramagnetic resonance; LUVET, large unilamellar vesicles by extrusion techniques; MLV, multilamellar vesicles; NBD-PE, *N*-(7-nitro-2,1,3-benzoxadiazol-4yl)-phosphatidylethanolamine; α-THS, alpha-tocopherol hemisuccinate.

0009-3084/90/$03.50

the bilayer phase was marked by the appearance of non-bilayer structures.

α-THS is a branched single chain lipid that differs dramatically in structure from other lipids such as phosphatidylethanolamine (PE) [5—7], cardiolipin and mono-diacyl glycerides [8] known to exhibit structural polymorphism. The factors affecting the polymorphism of this unusual bilayer forming lipid can thus be used to identify parameters governing the stabilization of non-bilayer lipid phases in general [9—11].

Materials and methods

Chemicals

α-Tocopherol hemisuccinate (α-THS), tocopherol, and Tris (Trizma Base) were obtained from Sigma (St. Louis, MO). *N*-(7-nitro-2,-1,3-benzoxadiazol-4yl)-phosphatidylethanolamine (NBD-PE), dioleoylphosphatidylethanolamine (DOPE), and lysophosphatidylcholine (lyso-PC) were obtained from Avanti Polar Lipids (Birmingham, AL). The methyl ester of 7-doxyl stearate was purchased from Molecular Probes (Eugene, OR).

Lipid and liposome preparation

The Tris salt of α-THS was prepared by mixing 2.28 g of Tris (Trizma Base, Sigma) dissolved in 2 ml of hot H_2O (the minimal amount of water required) to 10 g of α-THS dissolved in 100 ml of methylene chloride. The resulting mixture was dried first by rotary evaporation followed by further drying at 200 mTorr for 48 h at room temperature. The Tris salt of α-THS was used in all experiments, unless otherwise specified.

α-THS vesicles were formed by adding the dried powder to the appropriate buffer solution followed with periodic vortexing for two hours. For the tocopherol additions, α-THS and tocopherol were codissolved in methylene chloride, dried and liposomes formed as described above. For the kinetic experiments, 1 mol% NBD-PE was incorporated in the same manner as tocopherol but using chloroform/methanol as the solvent. The buffered solutions employed were either 50 mM glycine, 150 mM NaCl, pH 7.5 or 50 mM glycine, 50 mM citrate, 50 mM phosphate, 150 mM NaCl, at pH 7.5 or pH 10.5.

Formation of large unilamellar vesicles by extrusion (LUVETs) was performed as described previously [12]. Briefly, α-THS multilayered vesicles (MLVs) were made as above and passed four times through two stacked 400-nm polycarbonate filters (Nuclepore, Pleasanton, CA). The sample was then passed through 200-nm filters five times giving the $LUVET_{200}$ vesicles. For $LUVET_{100}$ vesicles an additional five passages through two stacked 100 nm filters was performed. The initial vesicle sizes were determined by freeze-fracture EM to be 100—700 nm for MLVs, 75—250 nm for $LUVET_{200}$ and 40—100 nm for $LUVET_{100}$.

Freeze-fracture electron microscopy

For freeze-fracture, a 0.1—0.3-μl aliquot of the specimen was removed from the lipid preparations or from the fluorometer at the appropriate time point and sandwiched between a pair of Balzers (Nashua, NH) copper support plates. These were incubated in a guillotine device employing an environmental chamber [13] and rapidly plunged into liquid propane. Samples were fractured and replicated on a double replicating device in a Balzers BAF 400 freeze-fracture unit at a vacuum of 5×10^{-7} mbar or better and at -115 °C. Replicas were viewed on a Philips 300 electron microscope at magnifications of 7,000 to 45,000 times.

Fluorescence

Fluorescence and light scattering measurements were performed on a PTI fluorometer (PTI Inc., Princeton, NJ). The NBD fluorescence assay for determining bilayer to non-bilayer transitions [14—16] was employed. In this assay, an increase in the fluorescence intensity of NBD is attributed to hexagonal phase formation. Excitation and emission were monitored at 465 nm and 544 nm, respectively. The change in the absolute fluorescence intensity with time was recorded following the addition of a 30-μl aliquot of 20 mM α-THS into 3 ml of the appropriate buffer with constant stirring,

unless otherwise specified. The contribution made by vesicle scattering was similarly recorded and subtracted using vesicles void of probe. Fluorescence intensities were relative to the pH 7.5 value at the corresponding temperatures. For light scattering measurements the signal was recorded at 90 degrees in arbitrary units by setting both monochromators at 450 nm.

X-ray

X-ray diffraction intensity versus scattering angle experiments were performed using the two-dimensional image intensified X-ray detector apparatus as described earlier [17].

Electron paramagnetic resonance

α-THS (30—50 mg/ml) was hydrated in a solution containing 50 mM glycine, 50 mM phosphate, 50 mM citrate and 150 mM NaCl. This combination of buffers was necessary in order to control uniformly the pH over the range used (pH 2 to 10). The methyl ester of 7-doxyl stearate was dried from an ethanol stock solution and the α-THS vesicle suspension added to it. The final label content never exceeded 1 mol%. For the pH titration, 1 M HCl was added and the samples allowed to stand (with periodic vortexing) at least 1 h before examination. Samples were placed into capillary tubes and the electron paramagnetic resonance (EPR) spectrum taken using a Bruker ER-100D Spectrometer equipped with an ER-4111VT Variable Temperature Controller (Bruker Instruments Inc., Billerica, MA).

Results and discussion

To assure complete charge neutralization, the pH of multilayered α-THS liposomes (Fig. 1A) was decreased from 7.5 to 2. Freeze-fracture microscopy of the precipitate that formed (Fig. 1B) revealed the presence of numerous tubes the dimensions of which were consistent with what has been observed for hexagonal II phase lipid [18]. Subsequent X-ray diffraction of the precipitate confirmed a two-dimensional hexagonal lattice with a 82.8-Å unit cell (Fig. 2). To explore whether this system was hexagonal II (rather than hexagonal I) we performed a series of experiments based upon the observation that hexagonal (H_{II}) forming lipids such as egg PE or DOPE can be stabilized into bilayers by the addition of lipids which normally form micelles, such as detergents and lysophosphatidylcholine [19,20]. Such stabilization presumably occurs due to shape complementarity. We prepared 1:1 mixtures of DOPE/α-THS and lyso PC/α-THS at pH 7.5 and subsequently incubated these systems in glycine buffer at pH 2.0. At pH 2 the DOPE/α-THS mixture formed a precipitate which by freeze-fracture revealed numerous tubes reminiscent of pure α-THS at this pH (data not shown). On the other hand at pH 2 the lyso PC/α-THS mixture remained vesicular (Fig. 1C) confirming that α-THS in fact forms hexagonal II phases at low pH. At intermediate pH values α-THS exhibited mixtures of bilayer and non-bilayer phases (Fig. 3) consistent with the bilayer to lipidic particle to hexagonal II phase transition seen for many diacyl lipid systems exhibiting polymorphism [4—7].

The rate of the pH induced transition was determined by NBD-PE fluorescence and freeze-fracture and found to be temperature dependent (Fig. 4). An obvious increase in the rate of hexagonal phase formation at pH 4.5 was observed as temperature was increased from 25 to 50°C. This is consistent with what has been reported for diacylphospholipids and has been attributed to an increase in the rotational mobility of the hydrophobic portions of the molecule. The transition also revealed a strong size dependence. Smaller vesicles ($LUVET_{100}$ and $LUVET_{200}$) tended to aggregrate and form non-bilayer phases more rapidly than MLVs. Since the surface area available for interaction is greater in smaller systems these results support the notion that bilayer contact is essential for non-bilayer phase formation. Alternatively, it is conceivable that the increased radius of curvature of the smaller vesicles played a role in the H^+-induced destabilization process. Freeze-fracture studies performed at one minute time points confirmed the fluorescence results. In fact, hexagonal phases occurred only where vesicle contact was apparent (Fig. 5a) as has been previously

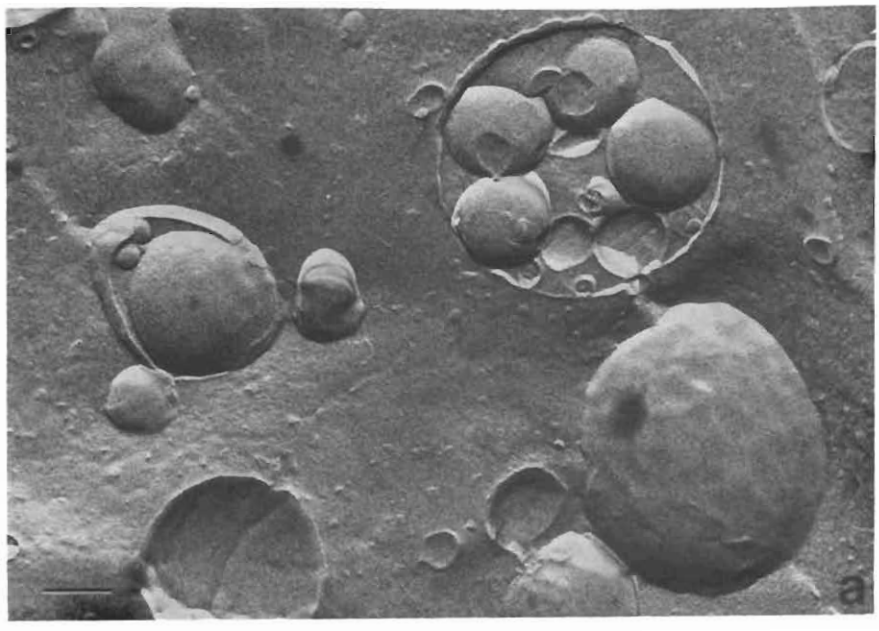

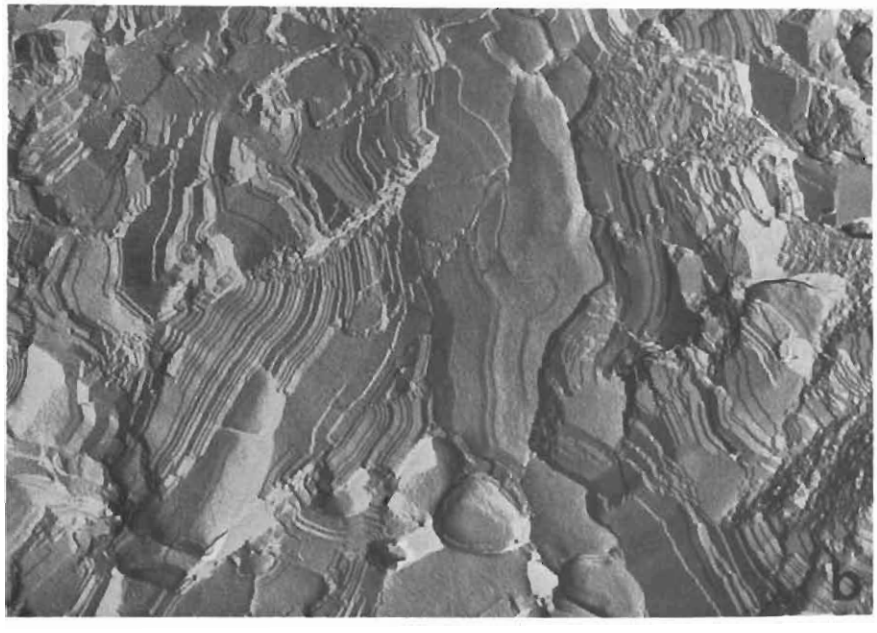

suggested [21]. At lower pH values the existence of non-bilayer phases was more extensive. For instance, the $LUVET_{100}$ specimen at pH 3.5, an obvious fusion product, revealed subtle striations among an amorphous phase, although some order in the form of cubic packing was visible (arrow) (Fig. 5b). All samples formed hexagonal phase following a two-hour incubation.

In the course of seeking a more quantitative

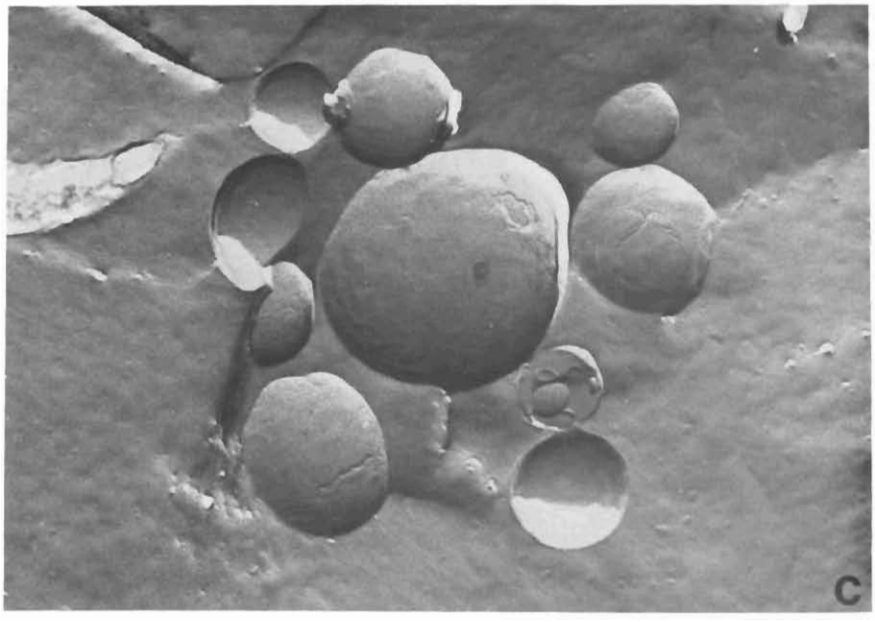

Fig. 1. (a) Freeze-fracture electron micrographs of an α-THS (Tris) dispersion in 50 mM tris buffer pH 7.5. (b) Prepared at pH 7.5 and diluted 1:100 in 50 mM glycine buffer pH = 2.0. (c) Prepared as in (B) but with 50 mol% lyso PC. Final concentration of all samples was 2 mM. All specimens were quenched from 25°C. In all the samples investigated no chemical breakdown could be linked to structural changes; all were found to >99% pure by HPLC following overnight incubations at the pH values employed. Bar = 0.2 μm.

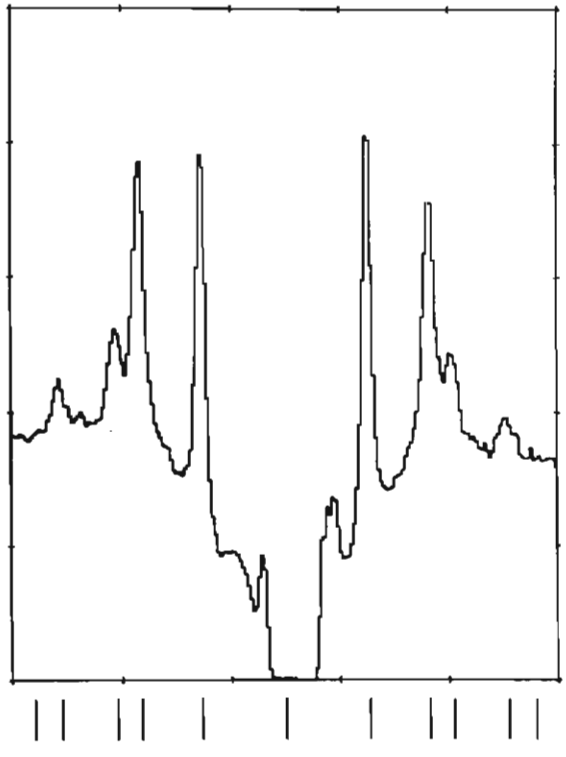

assessment of the pH induced transition we examined the electron paramagnetic resonance (EPR) spectra of several spin label species incorporated into α-THS vesicles. The most notable change was found with the methyl ester of 7-doxyl stearate (7-DS) which underwent an increase in A_{max} of 3—7 Gauss at the lower pH values (see Fig. 6). From an EPR study at −150°C this change was attributed to differences in the motional freedom of the probe and not the polarity of the probe environment (data not shown). Presumably the nitroxide group of this probe resides near the bilayer interface where an increase in the packing density of the lipid headgroups and interfacial region might be

Fig. 2. X-ray diffraction intensity (ordinate: arbitrary units) versus scattering angle (abscissa) for a 2 mM α-THS dispersion at pH 2 in glycine buffer at room temperature. The dip in the center of the graph is due to the X-ray beam stop shadow zero scattering angle. The tick marks below the graph indicate the expected positions of peaks from a 2-dimensional hexagonal lattice with an 82.8-Å unit cell.

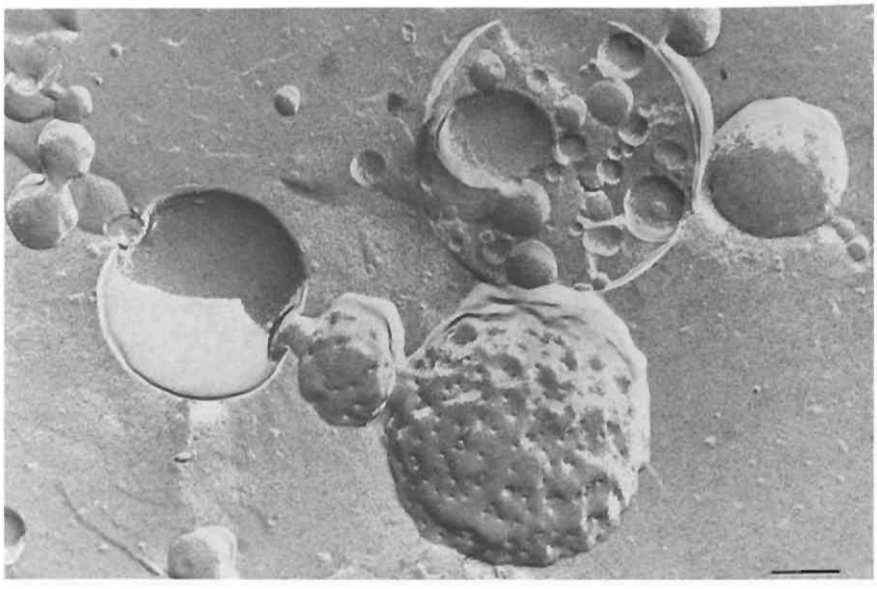

Fig. 3. Freeze-fracture electron micrograph of α-THS (50 mg/ml) at pH 6.8 rapidly frozen from 25 °C. Bar = 0.02 μm.

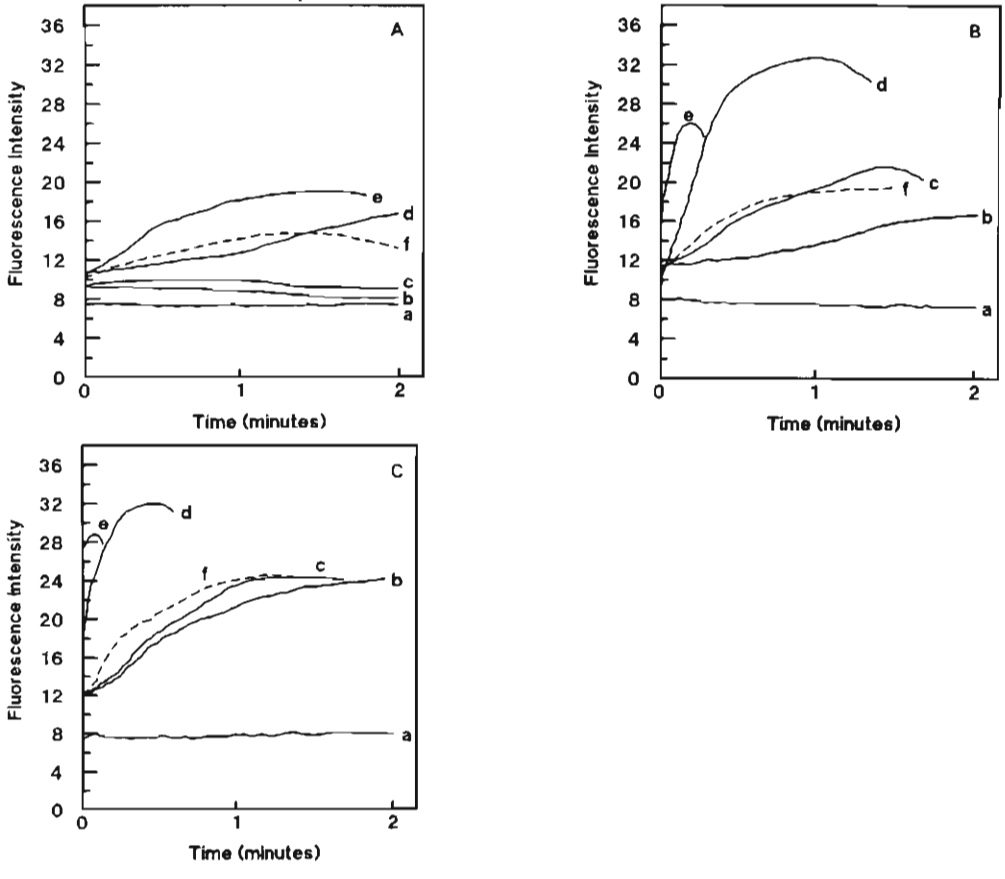

Fig. 4. The time course of NBD-fluorescence increase in α-THS liposomes at 0.2 mM and pH 4.5 as a function of vesicle size and temperature for (A) MLV, (B) $LUVET_{200}$ and (C) $LUVET_{100}$ at (b) 10 °C, (c) 25 °C (d) 35 °C, (e) 50 °C and (f) 25 °C at pH 3.5. (a) represents the baseline fluorescence.

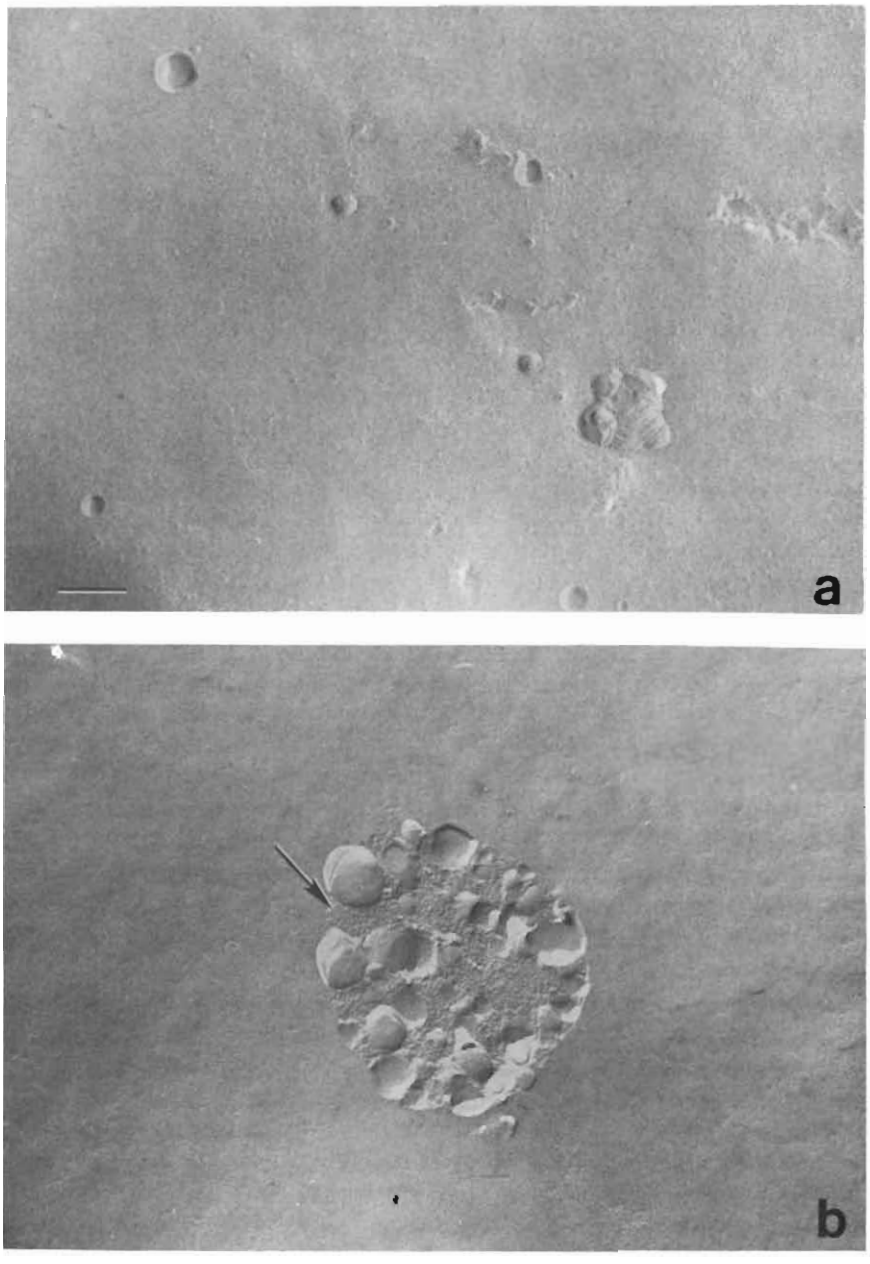

Fig. 5. Freeze-fracture electron micrographs of α-THS (a) $LUVET_{100}$ at pH 4.5 and (b) $LUVET_{100}$ at pH 3.5. Both samples were rapidly frozen at 1 min from 25°C. Bar = 0.2 μm.

expected upon protonation of the succinate. In any case, the transition marked by the probe was consistent with that found by freeze-fracture EM. Even though the magnitude of the change in A_{max} increased at higher temperatures the pH values marking the beginning and end of the transition remained unchanged indicating no temperature induced transition occurred over this range. Again this was consistent with the EM results. At the high lipid concentrations employed in these studies (75 mM) the transition was immediate and stable for over 6 h.

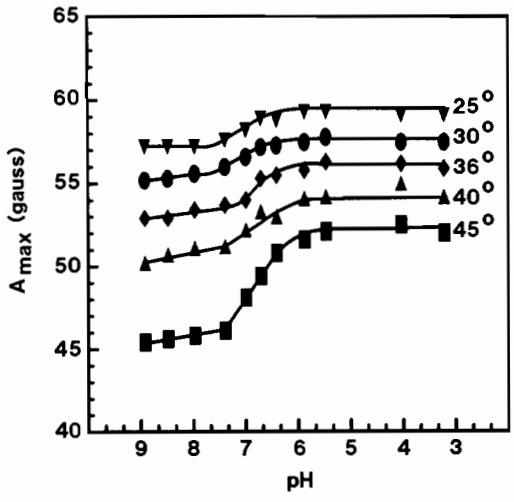

Fig. 6. A_{max} for the 7-DS spin probe (at 1 mol%) in α-THS vesicles (50 mg/ml) is shown. A_{max} is defined as the separation between the first maximum and the last minimum of the EPR spectrum (22). The buffer solution contained 50 mM citrate, glycine and phosphate with 150 mM NaCl. The samples were brought to the indicated pHs using 1 M HCl. When samples were made up at the pHs indicated the profile was identical. The effect of temperature upon pH was found to be negligible.

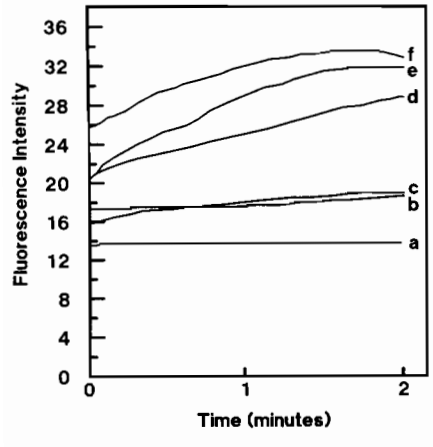

Fig. 7. The time course of the NBD-fluorescence increase in α-THS liposomes at pH 7.5 as a function of Ca^{2+} concentration (a) 0 mM, (b) 0.5 mM, (c) 1.25 mM, (d) 2.5 mM, (e) 5.0 mM and (f) 10.0 mM. α-THS concentration was held constant at 0.2 mM.

Hexagonal II phases have been induced in other negatively charged lipid species such as cardiolipin [23—26] and phosphatidic acid [27] by the addition of calcium. Accordingly, we investigated the effect of Ca^{2+} on α-THS by both NBD fluorescence and freeze-fracture EM at pH 7.5. As shown in Fig. 7 for α-THS MLVs, at the physiological concentration of 0.5 mM Ca^{2+}, a slow steady increase in the fluorescence intensity was observed. Concentrations of 2.5 mM Ca^{2+} and higher led to a rapid increase in fluorescence, the initial increase being too rapid to measure. Freeze-fracture replicas following a one-minute incubation of the 5 mM sample exhibited vesicles containing what appeared to be hexagonal tubes along with some large fusion products. The hexagonal tubes (Fig. 8A) appeared to result from the fusion of internal lamellae as opposed to the fusion between different vesicles. When $LUVET_{100}$ were employed, the formation of putative hexagonal phase was accelerated (results not shown). When α-THS MLVs were incubated for 10 min in 5 mM Ca^{2+}, freeze-fracture microscopy revealed the presence of systems comprised of bundles of tube-like structures (Fig. 8B). These systems were of the order of 0.5 μm or greater in diameter. Also present were large, multilamellar vesicles with tightly packed layers some of which also contained the tube-like structures. The vesicles themselves were angular in shape much like gel state lecithins in the presence of a dehydrating agent. Screw dislocations or line defects were also seen in these samples again reminiscent of dehydrated lamellar systems [28]. In fact if the Ca^{2+} incubation was allowed to progress past 10 min the dehydrated lamellar phase became predominant. Such a phase could account for the increase in NBD-PE fluorescence reported in Fig. 7.

These results were supported by subsequent X-ray studies. Small angle X-ray diffraction of the Ca^{2+} α-THS system (pH 7.5) after 10 min of incubation revealed a single broad band of scatter corresponding to a 50-Å repeat. This evolved to a single sharp band corresponding to a 51-Å repeat in two hours. That X-ray diffraction did not reveal a hexagonal lattice was most likely

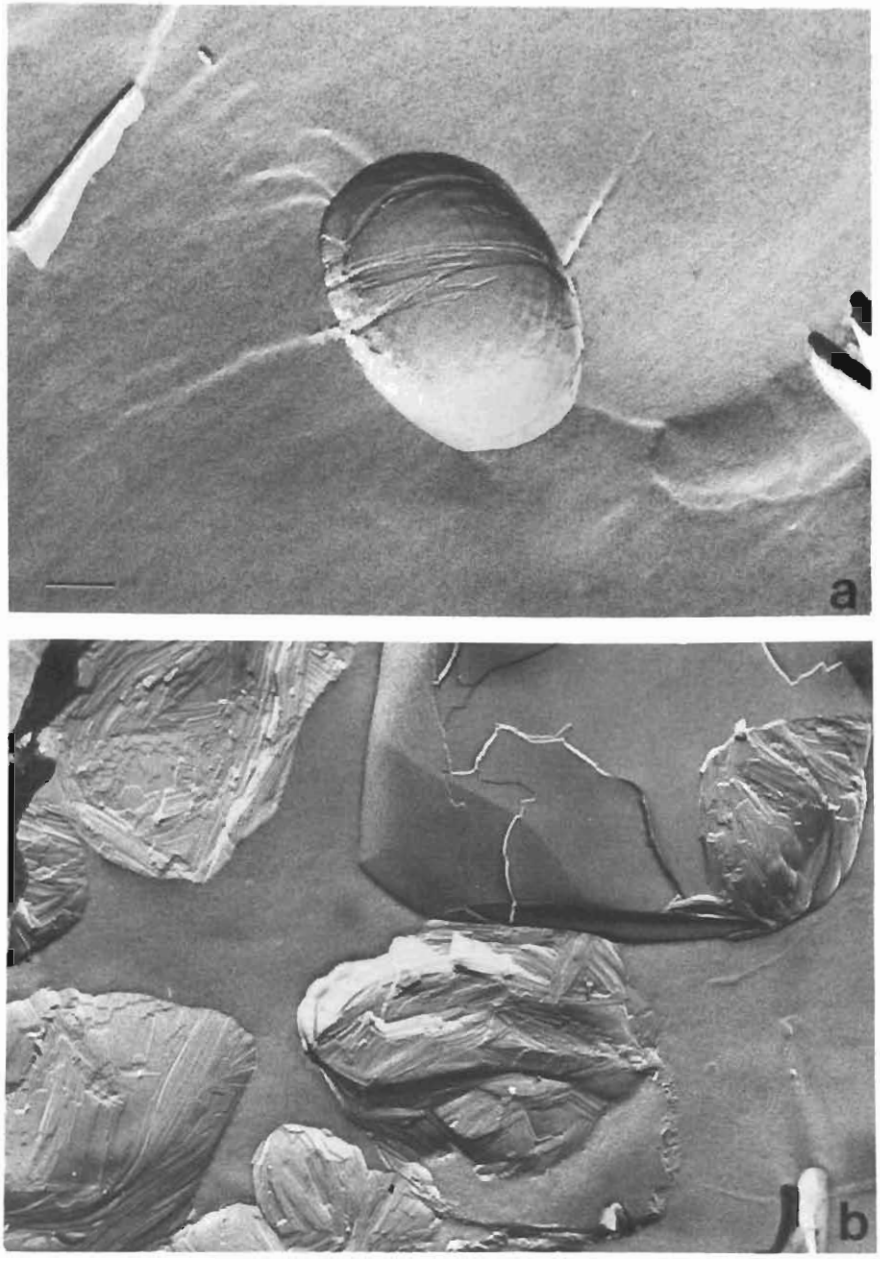

Fig. 8. Freeze-fracture electron micrograph of α-THS at pH 7.5 in 5 mM Ca^{2+} at 25°C (a) following a 1-min incubation and (b) following a 10-min incubation. Bar = 0.2 μm.

due to the rapidity of the transition to the dehydrated lamellar form. The fact that higher order scatterings were not present is consistent with a rigid lattice structure. These orders are known to be generally weak in gel state lipid.

Since it is charge neutralization of α-THS that appears to promote the bilayer to hexagonal phase transition, we began an investigation of the effect of tocopherol upon α-THS vesicles. We believed that this neutral molecule, possess-

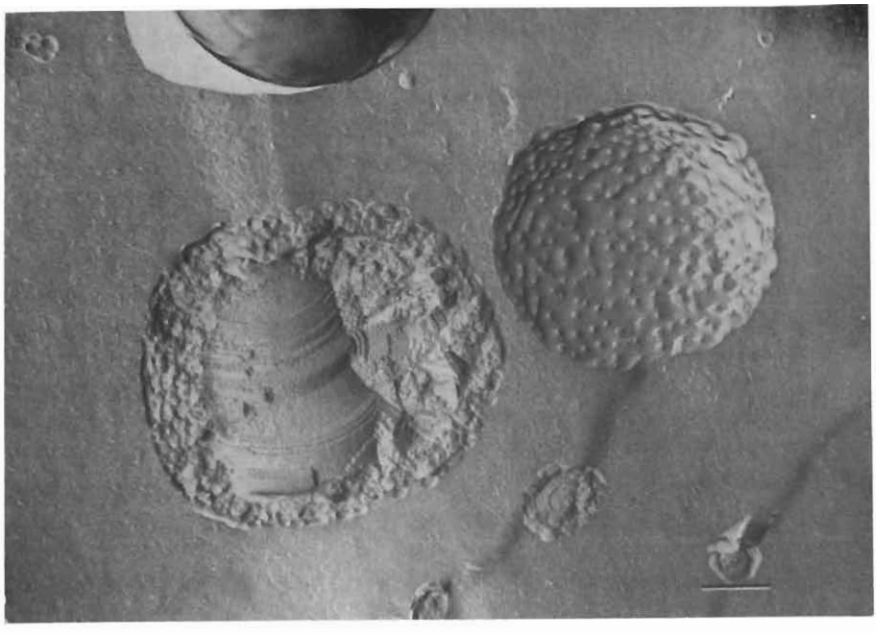

Fig. 9. Freeze-fracture electron micrograph of tocopherol/α-αTHS at a 4:6 mole ratio rapidly frozen from 25°C. Bar = 0.2 μm.

ing a small headgroup, would affect the polymorphic phase behavior of α-THS in a manner similar to protonated α-THS. From examination of freeze-fracture replicas of samples at pH 8.5 containing 0, 20, 30, 40, and 50 mol% tocopherol we found nonbilayer phases first occurring at 30% with the appearance of lipidic particles. These become more prevalent in the 40% system, as shown in Fig. 9, where hexagonal phase is shown enclosed within vesicles. At 50% tocopherol, only large clusters of hexagonal phase tubes were observed (data not shown). Thus, tocopherol can in fact promote the formation of extended non-bilayer phases in α-THS.

We have shown that α-THS can undergo a polymorphic phase transition that is induced at pH values below 7.5. This transformation appears to be the inverted hexagonal (H_{II}) phase resulting from the packing of presumably cone-shaped molecules [29]. Most likely the isoprene tail which forms the hydrocarbon core of the α-THS bilayer is able to contribute to this cone shape when the succinate head group region is condensed either by protonation or binding of Ca^{2+}.

The Ca^{2+} dependent headgroup dehydration of α-THS was found to lead to the formation of rigid, crystalline-like structures. This effect has been observed in PS systems, which at low pH can be induced to form hexagonal (H_{II}) phases but upon the addition of Ca^{2+} at neutral pH form a "rigid lattice" [30,31]. That Ca^{2+} and low pH induced different polymorphic forms in α-THS suggest that a complex interaction between dehydration and charge neutralization may be at play. Given the high charge density of α-THS liposomes, it is expected that the surface pH be lower than the bulk pH. Reduction of the αTHS surface charge density by inclusion of other lipids should also allow for modulation of the pH induced transition [21]. Although the details of numerous structural changes of α-THS are yet to be worked out, that they occur at all in this unique lipid should allow further elucidation of the factors underlying lipid structural polymorphism in general.

Acknowledgments

This work was supported by The Liposome Company, Inc., Princeton, New Jersey, U.S.A.

References

1 A.S. Janoff, C.L. Kurtz, R.L. Jablonski, S.R. Minchey, L.T. Boni, S.M. Gruner, P.R. Cullis, L.D. Mayer and M.J. Hope (1988) Biochim. Biophys. Acta 941, 165—175.
2 A.S. Janoff, L.E. Bolcsak, A.L. Weiner, P.A. Tremblay, M.V.W. Bergamini and R.L. Suddith (1987) Patent Cooperation Treaty Publications Number W08702219.
3 M.Z. Lai, N. Düzgünes and F.C. Szoka (1985) Biochemistry 24, 1646—1653.
4 C.P.S. Tilcock (1986) Chem. Phys. Lipids 40, 109—125.
5 P.R. Cullis and B. DeKruijff (1978) Biochim. Biophys. Acta 507, 207—218.
6 S.W. Hui, T.P. Stewart and L.T. Boni (1983) Chem. Phys. Lipids 33, 113—126.
7 R. Van Venetie and A.I. Verkleij (1981) Biochim. Biophys. Acta 645, 262—269.
8 K. Larsson, K. Fontell and N. Krog (1980) Chem. Phys. Lipids 27, 321—328.
9 J. Connor and L. Huang (1985) J. Cell Biol. 101, 582—589.
10 C.-Y. Wang, K.W. Hughes and L. Huang (1986) Plant Physiol. 82, 179—184.
11 M.B. Yatvin, I.-M. Tegmo-Larsson and W.H. Dennis (1987) Methods Enzymol. 149, 77—87.
12 M.J. Hope, M.B. Bally, G. Webb and P.R. Cullis (1985) Biochim. Biophys. Acta 812, 55—65.
13 R.M. Epand, R.F. Epand, T.P. Stewart and S.W. Hui (1981) Biochim. Biophys. Acta 649, 608—615.
14 H. Ellens, J. Bentz and F.C. Szoka (1986) Biochemistry 25, 285—294.
15 K. Hong, P. Baldwin, T. Allen and D. Papahadjopoulos (1985) Biochemistry 27, 3947—3955.
16 C.D. Stubbs, B.W. Williams, L.T. Boni, J.B. Hoek, T.F. Taraschi and E. Rubin (1989) Biochim. Biophys Acta 986, 89—96.
17 S.M. Gruner, R.P. Lenk, A.S. Janoff and M.J. Ostro (1985) Biochemistry 24, 2833—2842.
18 L.T. Boni and S.W. Hui (1983) Biochim. Biophys. Acta 731, 177—187.
19 R.P. Rand, W.A. Pangborn, A.D. Purdon and D.O. Tinker (1975) Can. J. Biochem. 53, 189—195.
20 T.D. Madden and P.R. Cullis (1982) Biochim. Biophys. Acta 684, 149—153.
21 H. Ellens, J. Bentz and F.C. Szoka (1984) Biochemistry 23, 1532—1538.
22 O.H. Griffith and P.C. Jost (1976) in: L.J. Berliner (Ed.), SPIN LABELING Theory and Applications, Academic Press, New York, pp. 453—523.
23 R.P. Rand and S. Sengupta (1972) Biochim. Biophys. Acta 255, 484—492.
24 W.J. Vail and J.G. Stollery (1979) Biochim. Biophys. Acta 551, 74—84.
25 P.A. Cullis, A.J. Verkleij and P.H.J.Th. Ververgaert (1978) Biochim. Biophys. Acta 513, 11—20.
26 B. DeKruijff, A.J. Verkleij, J. Leunissen-Bijvelt, C.J.A. Van Echteld, J. Hille and H. Rijnbout (1982) Biochim. Biophys. Acta 693, 1—12.
27 D. Papahadjopoulos, W.J. Vail, W.A. Pangborn and G. Poste (1976) Biochim. Biophys. Acta 448, 265—283.
28 L.T. Boni, T.P. Stewart and S.W. Hui (1984) J. Membrane Biol. 80, 91—104.
29 S. Nir, J. Wilschut and J. Bentz (1982) Biochem. Biophys. Acta 688, 275—278.
30 M.J. Hope and P.A. Cullis (1980) Biochem. Biophys. Res. Comm. 92, 846—852.
31 A. Kim, H. Ellens, J. Bentz and F.C. Szoka (1987) Biophys. J. 51, 356a.